UNITED NATIONS UNIVERSITY
GEOTHERMAL TRAINING PROGRAMME
Orkustofnun, Grensasvegur 9,
IS-108 Reykjavik, Iceland

Reports 2012
Number 18

COOLING SYSTEM DESIGN FOR A BINARY POWER PLANT IN NORTH-GOUBHET FIELD, DJIBOUTI

Abdoulkader Khaireh Allaleh
Ministry of Energy
Cite Ministériel
P.O. Box 10010
DJIBOUTI
khaireh.abdoulkader@gmail.com

ABSTRACT

Binary plants represent around 10% of the total installed capacity of geothermal plants. Technology has improved in the last decades and permits low- and medium-temperature geothermal field exploitation for power generation. Different configurations are available ranging from a simple binary cycle, or a stand-alone cycle, to combinations with a flash cycle or a bottoming cycle. Due to low efficiency, between 10 and 13%, and high investment capital, binary plant implementation has been limited. To increase the net output and plant efficiency, the design of a cooling system is analysed and its effects on power production are studied. Three systems are used for cooling, i.e. water cooling, wet cooling, and dry cooling, depending on different parameters like water availability, weather data, etc. In the report, designs of a cooling system are studied using data from the North-Goubhet geothermal field in Djibouti.

1. INTRODUCTION

The Republic of Djibouti has considerable geothermal potential. It is estimated at around 800 MW, mainly located in the Lake Asal region. Several surface studies and exploratory drilling have verified the potential of this area, which is divided into two geothermal fields, Asal geothermal field and North-Goubhet geothermal field (Jalludin, 2012).

In the North-Goubhet field (Figure 1), several studies have been done. In 1987, a survey was conducted by BRGM. The latest exploration effort was carried out in 2010 by CERD (Centre of Research Djibouti) for better assessment of this field. These exploration studies located three potential zones following the NW-SE trending axis of the geological structures, found by geophysical measurements and gravimetry. The chemistry of the geothermal manifestations showed a bicarbonate fluid with sodium and magnesium contents, and an estimated temperature of around 170°C.

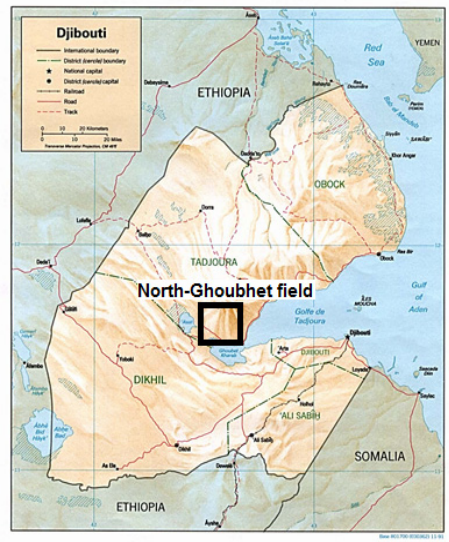

FIGURE 1: Location of the North-Goubhet field

Knowing the potential of the field and the estimated temperature, a binary power plant was found to be the best solution for power production, as indicated in the Lindal diagram. A cooling system is an important part of this power plant design, because of the high ambient temperature of the field and the lack of available water in the area.

After presentation of the geothermal field and binary plant technology, the focus of the study will be on a cooling system design, based on the climatic conditions of the North-Goubhet field.

2. STATUS OF NORTH-GOUBHET GEOTHERMAL FIELD

The Republic of Djibouti, with a surface area of 23,000 km², is located in East Africa where three major extensional structures, the Red Sea, the East African rifts and the Gulf of Aden, join to form the Afar depression (Barberi et al., 1975).

The Afar depression part of Djibouti is characterized by the presence of geothermal resources, revealed by numerous hot springs and fumaroles found in different parts of the country. The most active structure is the Asal Rift which is the westward prolongation of the Aden Gulf. It has a NW-SE trend and submerges in a southeast direction into the Goubhet Gulf and in a northeast direction into Lake Asal (155 m below sea level, the lowest point in Africa).

2.1 Geothermal exploration

The North-Goubhet field (Figure 1) is located to the northeast of the Asal high-temperature field and is correlated with different geological structures; it is also very active. Interest in this field started in 1987, when exploration studies were done in the Asal field, as the North-Goubhet area is close to the Asal rift. Goda Mountain and the Makarassou region are found in the northern part while the study zone is limited by the sea in the south. The elevation of the geothermal area reaches up to 500 or 600 m above sea level.

2.2 Geology

Figure 2 shows a geological map of the North-Goubhet area. The area is situated between zones of different tectonic patterns and is, therefore, affected by several tectonic trends: the Asal rift NW-SE faults, the Makarassou N-S trends (Tapponnier and Varet, 1974) and old trends identified in the Goda Mountain. Tectonic activities are clearly revealed in the area, confirmed by some faults seen in recent sediments and large panels of steep cliffs formed in the Dalha basalts. Along the scarped valleys of the "wadis", several fumaroles and one boiling spring are found at the bottom of the volcanic cliffs.

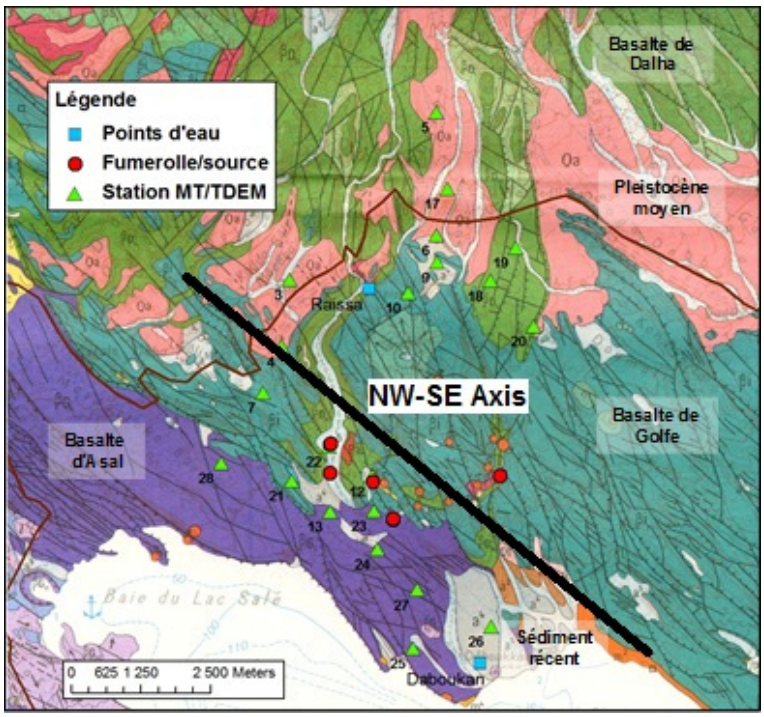

FIGURE 2: Geological map of the North-Goubhet area, Djibouti (CERD, 2010)

The geology is marked by the Dalha basaltic outcrops covered by more recent Gulf basalts and Pleistocene sediments. The basaltic rocks from Dalha are shown in green colour in Figure 2 and more recent basalts from the Gulf are in shown turquoise. The tectonic activities of the zone are controlled by fracture networks, trending NW-SE (Figure 2). A horst formation is observed in the field, a result of the tectonic activities and rifting (Figure 3). The Moudoueoud horst is covered by Gulf and Asal rift rock in the upper parts; while below, Dalha layer rocks are found. In the south in the coastal area, the geology is composed mainly of the Gulf basaltic rocks.

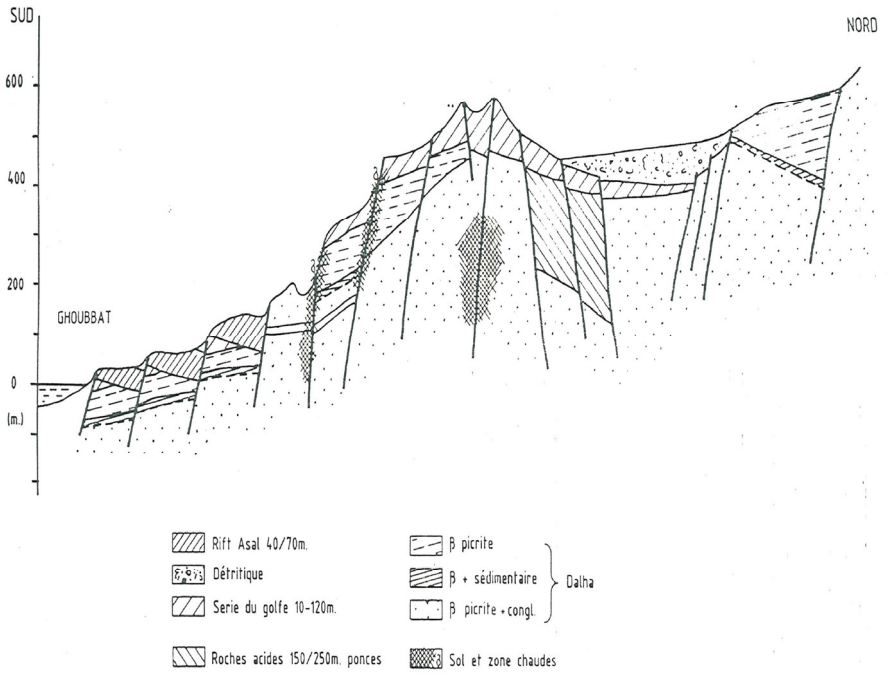

FIGURE 3: Geological cross-section (modified from CFG, 1985)

2.3 Geophysical measurements

Geophysical surveys were conducted in the early stages of exploration in the area of North-Goubhet. Gravimetry and AMT measurements were conducted by the French geological survey (BRGM) in 1983. The gravimetric results (Figure 4) point out several high and low gravity anomalies not distributed uniformly. However, these anomalies show different linear trends, which can be correlated to the tectonic activities of the area. In the study, three main zones were identified: in the southern Asal rift system, gravity lows were found; while in the northern zone, a large axis comprises a succession of gravity highs and lows; and in the central part, a similar axis was identified

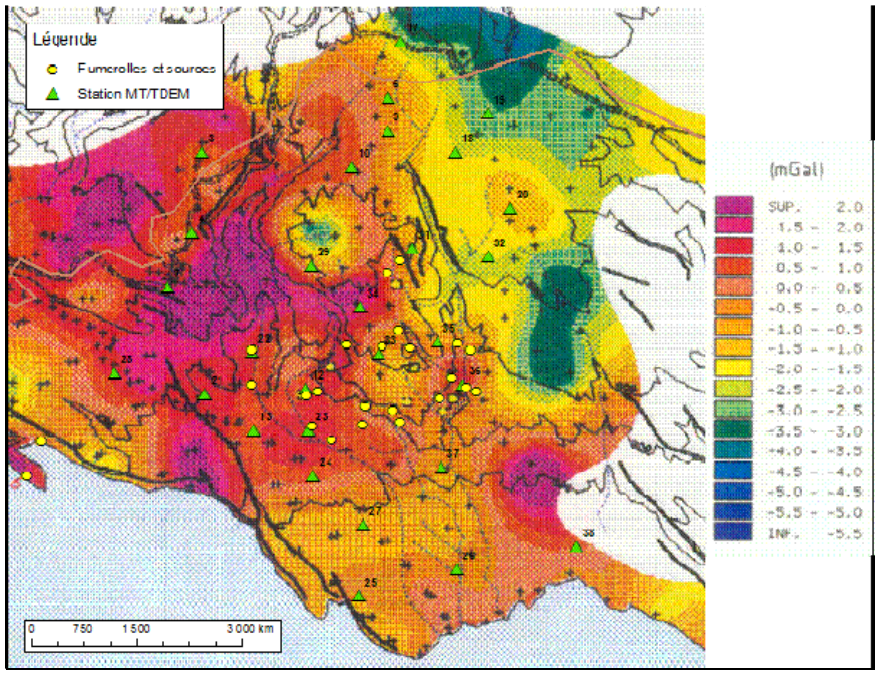

FIGURE 4: Gravity map (BRGM, 1983) and MT/TDEM stations measured by CERD in 2010

with a NNW-SSE trend. Hydrothermal activity is located along this NNW-SSE structure (yellow dots in Figure 4).

The 1983 survey also identified a conductive body in the central part of the field through the AMT measurements. It was estimated that the bottom of the conductive zone could be at around 1000 m depth. The AMT survey identified the prospect of an uplifted conductive body in the central zone. This study's identification of three main zones was confirmed through the resistivity anomalies.

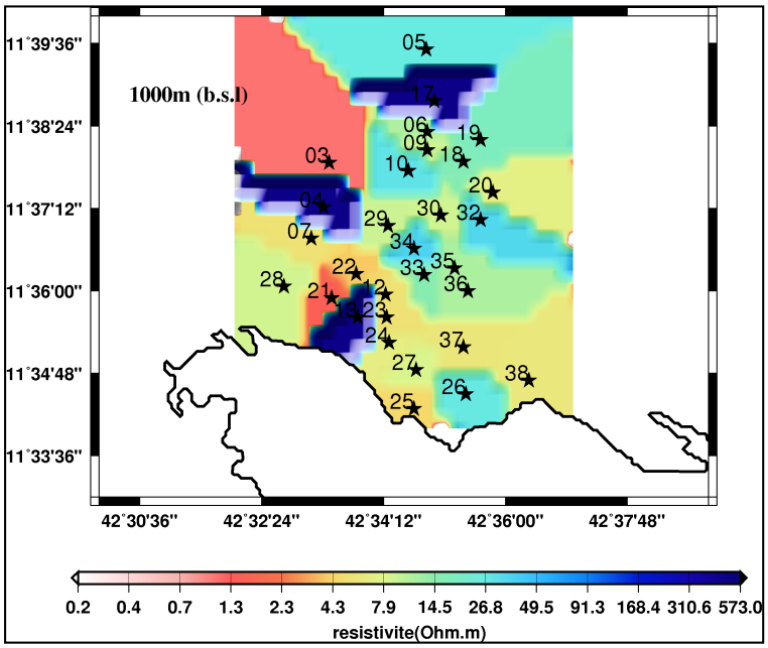

FIGURE 5: Resistivity map at 1000 m below sea level (CERD, 2010)

According to the subsequent recommendations of the 1983 study, CERD (Centre of Research of Djibouti) carried out an exploration study in the area in 2010. The CERD geophysical team conducted 30 MT (Magneto-Telluric) soundings and 26 TDEM (Time-Domain ElectroMagnetic) soundings. The electrical measurements show that in the uppermost few hundred metres, a conductive layer is dominant, but in the deeper zone, at 1000 m b.s.l. a heterogeneous body is found, with conductive anomalies which may be associated with hydrothermal fluids (Figure 5). At these depths, hydrothermal circulation is probably controlled by the main tectonic structures. The TDEM/MT data were used to construct several horizontal maps at different depths. Using all the different methods it was possible to localize the geothermal reservoir and the hydrothermal activity, including a low-resistivity zone below the Moudoueoud horst, confirmed by the MT measurements. The survey identified three main sites as having geothermal potential in the North-Goubhet field.

2.4 Geochemical measurements

A previous study in North-Goubhet field, done by the Italian company Geothermica in 1987, found a fluid with a different composition from the neighbouring field, Asal, with a less saline content. To add to this study, an exploratory survey by CERD was conducted in 2010, including sampling from different fumaroles around the three main zones defined by the survey, as well as from a wellbore. Different methods were applied to find the chemical composition of the geothermal fluids; such as the Piper diagram, geothermometers, and isotope analysis. These show that the primary steam does not come from undiluted or diluted deep water that exists in this system. Instead, the fumaroles are more likely to be the result of secondary steam from previously condensed steam or boiling groundwater (Geothermica, 1987).

In terms of alteration in the soil, a reddish alteration was seen around the fumaroles and assumed to be clay minerals from the geothermal fluids. The Piper diagram shows that the chemical composition of the geothermal fluid is mainly bicarbonate-calcite and magnesium, with a similar composition as a water sample from Goda Mountain. This gives an indication of the origin of the geothermal fluid.

The study also gave a possible reservoir temperature of between 100 and 170°C using the silica geothermometer, while other geothermometers, Na/K, Na/K/Ca, gave higher temperatures (CERD, 2010). However, to complete the measurements, more geochemical surveys are planned, using e.g. the CO_2 geothermometer and gradient well sampling, to find the actual temperature of the geothermal reservoir.

2.5 Reservoir modelling and planned surveys

The last exploratory study seems to confirm the potential of the North-Goubhet area and, consequently, it would be interesting to be able to confirm these results through drilling and exploitation of the resource. The 2010 survey also provided the basis for creation of a reservoir model of the geothermal system (Figure 6) which allowed delineation of a prospective area for exploration drilling in the area around the Moudoueoud horst. As seen in Figure 6, the geothermal reservoir is located below a large impermeable layer and the recharge water is controlled by a network of fractures, displayed by blue arrows from Goda Mountain and through orange arrows from the marine intrusion. According to the results of the gravimetric, TDEM, and MT measurements, sites for exploratory drilling were determined at the junction of the Bouguer anomaly and the low-resistivity zone expected to be a good area to access the geothermal reservoir. Furthermore, it can be added that directional drilling has been decided upon to be able to target and penetrate more feed zones in the reservoir.

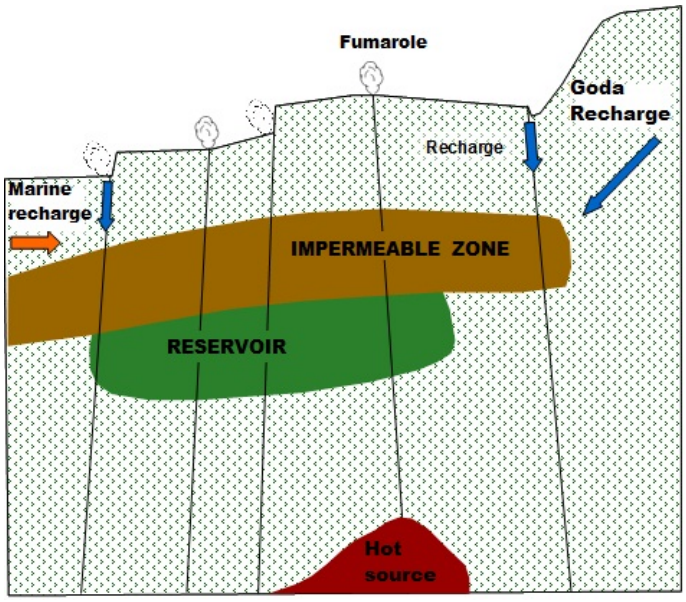

FIGURE 6: Conceptual model of the reservoir (CERD, 2010)

3. BINARY POWER PLANT CYCLES

3.1 Binary cycle overview

The Organic Rankin Cycle (ORC) is shown in Figure 7, with the working fluid operating in a closed-loop cycle, while the thermodynamic diagrams are shown in Figure 8. The cycle is composed of:

- Preheater PH (between points 1 and 2);
- Evaporator EV (between points 2 and 4);
- Turbine and generator (between points 4 and 5);
- Condenser (between points 5 and 7);
- Pump station for working fluids (between points 7 and 1).

The geothermal brine enters the system through heat exchangers, where heat is transferred to the working fluid. Basically, there are two stages in the heat exchanger, the first stage is the evaporator and the second is the preheater. Another heat exchanger is required to cool the working fluid. After being heated in the heat exchanger (preheater and evaporator), the working fluid goes to the bubble point, and is vaporized into steam inside the evaporator. After the vaporizing process, the steam goes directly to

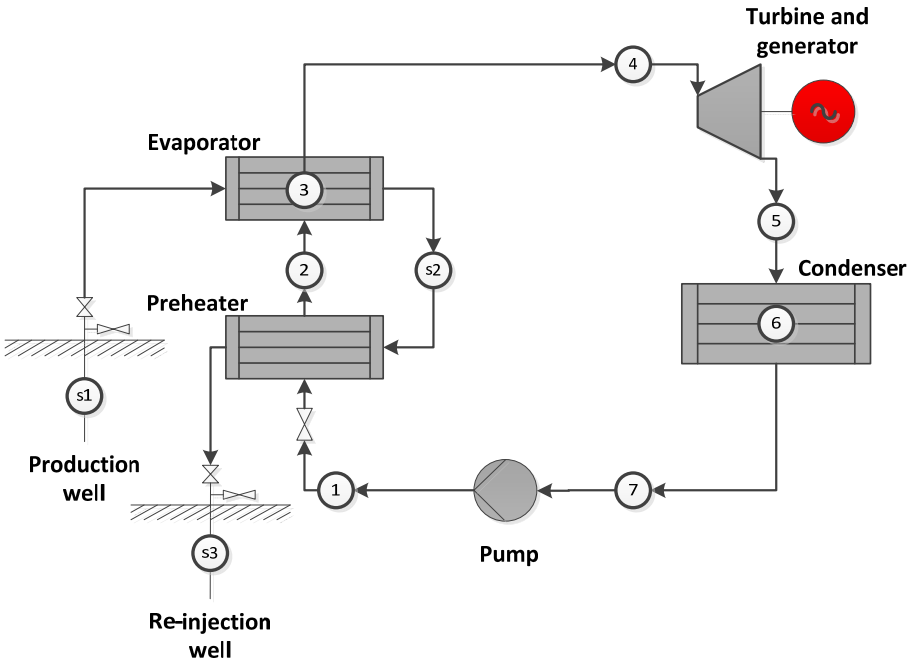

the turbine to convert thermal energy into mechanical energy. After passing through the turbine, the steam is condensed through a condenser from a steam phase into a liquid phase. After leaving the condenser, the working fluid enters the pump, where pressure is increased and the fluid goes through the heat exchanger to repeat the working cycle.

FIGURE 7: Schematic diagram of an ORC cycle

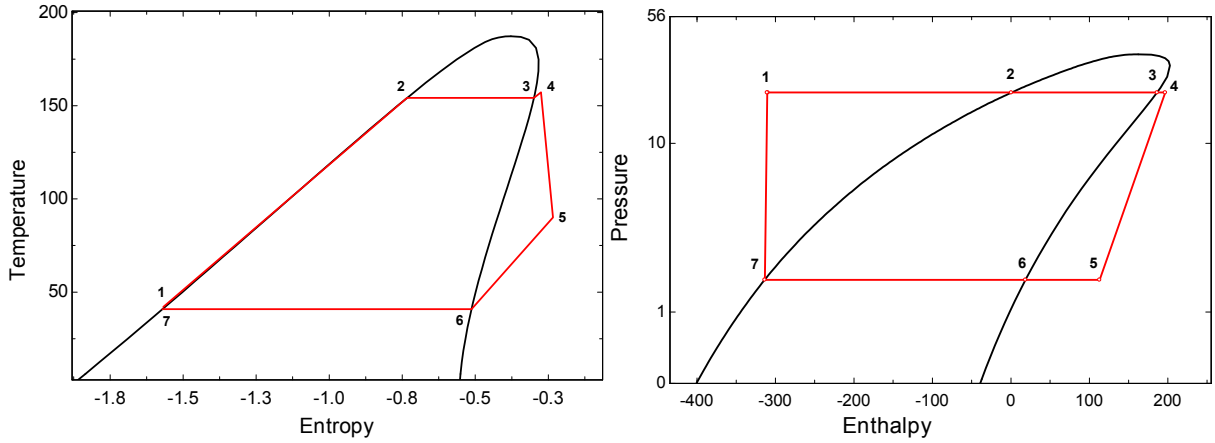

FIGURE 8: Temperature-entropy diagram and pressure-enthalpy diagram

3.2 Preheater and evaporator

A heat exchanger is used to transfer heat from the geothermal fluid to the working fluid. In this study, the heat-exchanger was composed of a preheater and an evaporator (Figure 9).

The preheater is a heat exchanger that heats the working fluid before it enters the evaporator. When the water approaches the boiling point, heat is added to evaporate the working fluid into saturated steam in the evaporator. From there the working fluid goes directly to the turbine.

A conventional heat exchanger is a shell and tube one, with an improved design aimed at reducing the overall size of the tube by finning, and containing the binary fluid on the shell side. Otherwise, heat performance would be reduced in the heat exchanger due to scaling problems caused by the chemistry of the geothermal fluid. Such scale reduces the heat transfer and hydraulic performance of a shell and tube heat exchanger and causes an increase in maintenance costs. Utilization of steam or pressurized

water and steam mixtures as a heat source provides a solution to the probable scaling problem in the heat exchanger as well as in the preheater or evaporator.

In order to find the thermodynamic relationship between the geothermal fluid and the working fluid, we assume some standard parameters:

- Steady-state operating conditions;
- Pure counter-current flow in heat exchangers;
- Constant overall heat transfer coefficient;
- Constant specific heat of the geothermal fluid.

The heat losses through the heat exchanger are neglected and the total amount of heat, Q added to the working fluid is equal to the heat extracted from the geothermal fluid. The following equations describe this:

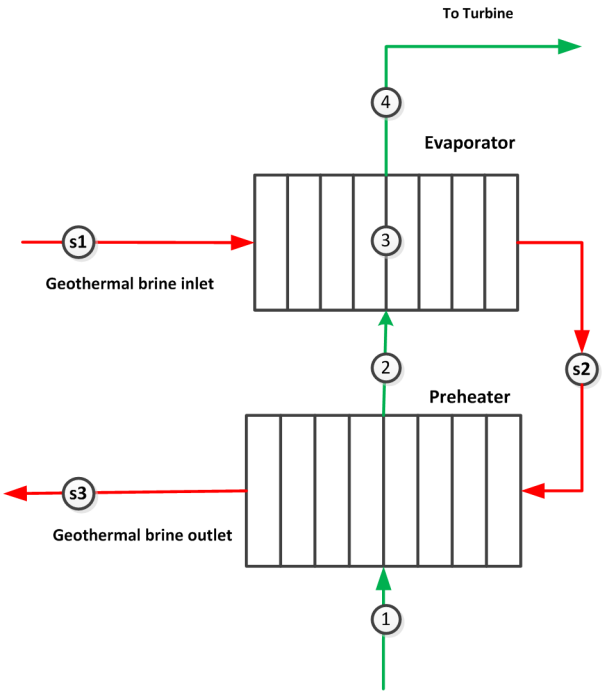

FIGURE 9: Schematic diagram of a preheater and an evaporator

$$Q = \dot{m}_{geo}(h_{s1} - h_{s3}) \quad (1)$$

$$Q = \dot{m}_{wf}(h_1 - h_4) \quad (2)$$

where $\dot{m}$ = Mass flow (kg/s);
h = Enthalpy (kJ/kg);
wf indicates the working fluid; and
geo indicates the geothermal fluid.

Hence the thermodynamic heat balance is:

$$m_{geo}(h_{s1} - h_{s3}) = m_{wf}(h_1 - h_4) \quad (3)$$

And in a case where the geothermal fluid contains low dissolved gases and solids, the previous equation becomes:

$$\dot{m}_{geo} * cp\ (T_{s1} - T_{S3}) = \dot{m}_{wf}(h_1 - h_4) \quad (4)$$

Based on the constant heat capacity of the heat source (geothermal fluid), the energy balance in the evaporator and the preheater can be described by the following equations where cp represents specific heat at constant pressure (Figure 9):

Evaporator: $$\dot{m}_{wf} * (h_4 - h_2) = \dot{m}_{geo} * cp(T_{S1} - T_{s2}) \quad (5)$$

Preheater $$\dot{m}_{wf} * (h_2 - h_1) = \dot{m}_{geo} * cp\ (T_{s2} - T_{S3}) \quad (6)$$

For designing an individual heat exchanger, it is important to look at the temperature distribution and heat transfer path diagram (Figure 10). The abscissa represents the heat transfer from the geothermal fluid to the working fluid, dependent on the temperature. The preheater gives sensible heat from the geothermal fluid to the working fluid before the working fluid goes to the evaporator.

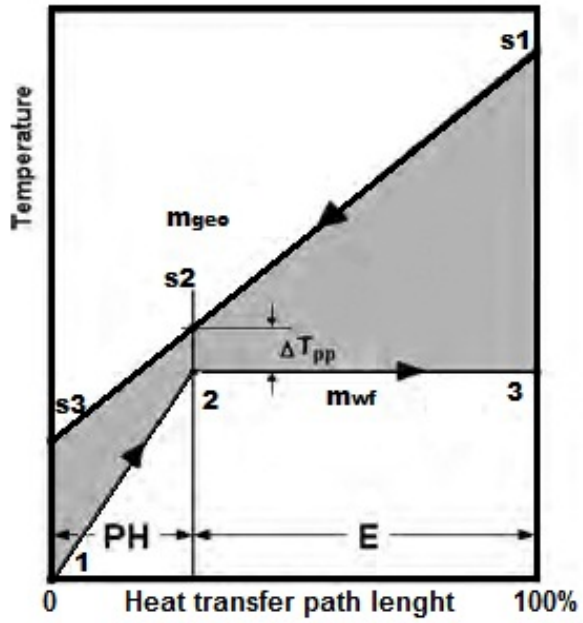

FIGURE 10: Preheater and evaporator temperature distribution (modified from DiPippo, 2008)

This diagram shows the heat transfer in the preheater PH, and the evaporator E. The pinch point ΔTpp is the minimum temperature difference between the geothermal fluid and the working fluid (DiPippo, 2008). The location of the pinch point and the value of the pinch point temperature difference are two major parameters influencing the performance of the heat exchanger. The pinch point temperature is generally known from the heat exchanger manufacturer's specifications. The total amount of heat transferred in the heat exchanger is found by the following equation (DiPippo, 2008):

$$Q = \mathrm{U} * \mathrm{A} * \mathrm{LMTD} \tag{7}$$

Where U = Overall heat transfer coefficient (W/m^2K);
A = Total heat transfer area (m^2);
LMTD = Logarithmic mean temperature difference (K).

LMTD can be calculated as follows:

$$\mathrm{LMTD} = \frac{(T_{hot,in} - T_{cold,out}) - (T_{hot,out} - T_{cold,in})}{\ln(\frac{T_{hot,in} - T_{cold,out}}{T_{hot,out} - T_{cold,in}})} \tag{8}$$

where the subscript *hot* refers to fluid which has a higher temperature, *cold* refers to the fluid with a lower temperature and subscripts *in* and *out* suggest the inlet and outlet of the heat exchanger.

3.3 Turbine and generator

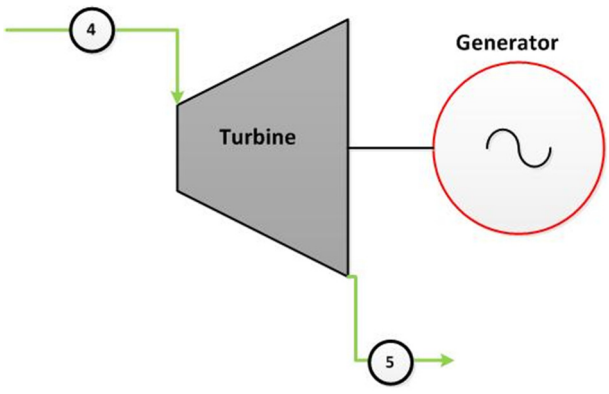

FIGURE 11: Schematic diagram of a turbine and a generator

The major role of the turbine is to convert the thermal energy from the working fluid into electrical energy through the generator (Figure 11). The turbine changes the potential energy of pressurized gasses into rotational kinetic energy. The vapour steam of the working fluid expands in the turbine, and leads to rotation. The rotor is connected by a shaft to the generator. The expansion process is considered adiabatic and steady state of the operation is assumed. The turbine is the main component of the power plant and the main device for transforming the thermal energy into electrical energy via the generator connected to it.

In power generation when the power plant is connected directly to the grid, the most used generator is asynchronous. The turbine has an isentropic efficiency (η_t) which is given by the manufacturer, and generated power can be calculated as follows in accordance with Figure 11 (DiPippo, 2008):

$$W_{turbine} = \dot{m}_{wf}(h_4 - h_5) \tag{9}$$

$$W_{turbine} = \dot{m}_{wf*}\eta_t(h_4 - h_{5s}) \tag{10}$$

where h_{5s} = Enthalpy of the fluid at the turbine outlet, assuming isentropic expansion (kJ/kg);
η_t = Efficiency of the turbine.

3.4 Feeding pump

In a binary power plant, several pumps are used in different parts of the system. Basically, the working fluid is pumped from the condenser to the preheater. Also pumps are located in the cooling system in a water cooling or wet cooling system. These pumps push the water or coolant fluid into the condenser. Pumps are also used for reinjection of brine or makeup water. The following equation is used to calculate the power needed to pump a certain amount of water $P_{pump\ motor}$ (Perry and Green, 2008):

$$P_{pump\ motor} = \frac{H * Q * g * \rho}{\eta_{pump} * \eta_{motor}} \tag{11}$$

For mass flow consideration:

$$P_{pump\ motor} = \frac{H * m * g}{\eta_{pump} * \eta_{motor}} \tag{12}$$

where $P_{pump\ motor}$ = Power of the motor driving the pump (W);
H = Pump head (m);
m = Mass flow (kg/s);
Q = Volume flow rate (m³/s);
ρ = Density of the coolant fluid (kg/m³);
g = Acceleration of gravity equal to 9.81 m/s²;
η_{motor}= Efficiency of the motor;
η_{pump} = Efficiency of the pump.

3.5 Fan motor

Most cooling towers used in geothermal plants are of a mechanical draft type, using a fan in both wet and dry cooling systems. The equation for calculating the power of the fan's motor is:

$$P_{fan\ motor} = \frac{(\frac{\dot{m}_{air}}{\rho_{air}}) * \Delta p}{\eta_{fan} * \eta_{fan\ motor}} \tag{13}$$

where $P_{fan\ motor}$ = Power of fan motor (W);
Δp = Pressure drop in the cooling tower (Pa);
$\dot{m}_{air}$ = Mass flow of the air (kg/s);
ρ_{air} = Density of the air leaving cooling tower (kg/m³);
η_{fan} = Efficiency of the fan;
$\eta_{fan\ motor}$= Efficiency of the fan motor.

3.6 Cooling systems

To improve the net output of the plant, it is important to develop a cooling system that cools the steam leaving the turbine. A good system can cool the working fluid to an optimal pressure and temperature and thus contribute to raising the net output of the power plant as well as controlling the reinjection temperature of the geothermal fluid. To achieve all this, there are different cooling systems which use either air or water as a heat sink or a mix of both. There are three types of cooling systems (Mendrinos et al., 2012):

1. Water cooling system;
2. Wet cooling system;
3. Dry cooling system.

3.6.1 Water cooling system

In the water cooling system exhaust steam from the turbine is condensed in a shell and tube heat exchanger (Figure 12). This is similar to the cooling system in a conventional thermal power plant. The main objective of the condenser is to convert steam into a liquid phase before pumping. The cooling water is transported to the condenser at the power plant using piping from a river, lake or sea. The range in water temperature is commonly between 5 and 25°C, depending on the season's temperature. For temperatures higher or lower than this, it may become difficult to use this kind of cooling system.

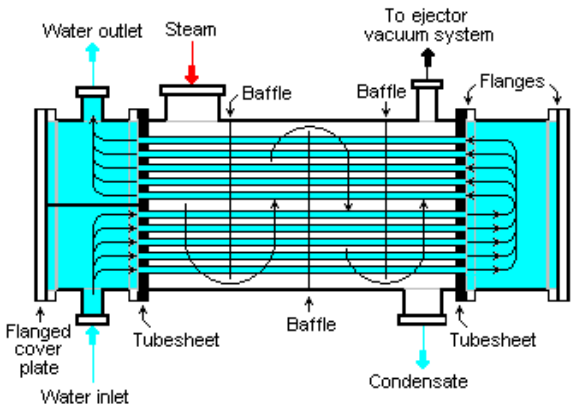

FIGURE 12: A water cooling condenser (Wikipedia, 2012)

This type of condenser is used when the power plant is located close to areas with good access to waters, but the main problem is the large amount of water needed, and the possible corrosion in the condenser due to the chemistry of the water. This system is used in the Reykjanes geothermal power plant in Iceland with seawater pumped from shallow boreholes in the coastal area.

3.6.2 Wet cooling system

A wet cooling tower system (Figure 13) is the most common cooling system in geothermal plants, using both water and air. This system is composed of a surface condenser which condenses the working fluid before entering the pump. While transferring heat to the cooling water, the working fluid changes phases and then goes directly to the pump.

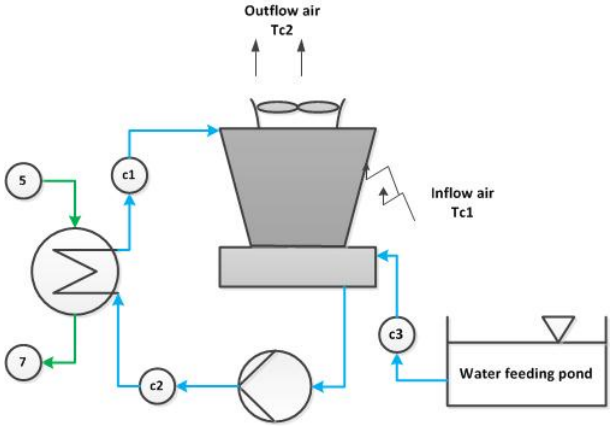

FIGURE 13: The wet cooling cycle

The main technology used in geothermal plants is mechanical draft induced with a fan, with two main tower configurations available, indicating the direction of the air flow in relation to the water flow:

- Counter flow;
- Cross flow.

In a wet cooling cycle, the coolant fluid (water) goes through the cooling tower (Figure 13) to dissipate heat stored in the surface heat exchanger. Passing through a cooling tower, the water, which runs gravitationally from the top of the tower, is cooled down by a fan, using the outside air. The supply of make-up water needed usually comes from groundwater but, in some cases, from a lake or seawater. A supply of make-up water (c3) is needed to compensate for evaporation losses. A wet cooling system is commonly used in many geothermal plants for high efficiency, but presents some disadvantages like the large amount of water needed, water vapour plumes and also some corrosion in the fan due to the chemistry of the water.

In wet cooling, the airflow is mechanically drafted with the fan. Most geothermal plants use an induced drafted fan on top of the tower, for a better cooling process. Figuring out the energy balance of the cooling tower requires complex equations due to the numerous parameters involved. The following steps summarize this process and the equations.

The mass balances inside a wet cooling tower take account of the air entering and leaving (Figure 14) as well as the water entering and leaving the condenser and the make-up water supply. The equations are:

Mass balance for dry air:

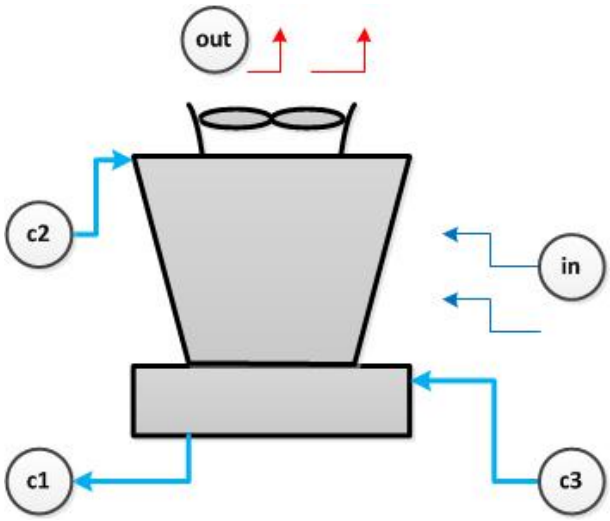

FIGURE 14: Cooling tower inflows and outflows

$$\dot{m}a_{in} = \dot{m}a_{out} = \dot{m}_{air} \tag{14}$$

Mass balance for water and the vapour content in the air stream:

$$\dot{m}v_{in} + \dot{m}_{c2} + \dot{m}_{c3} = \dot{m}_{c1} + \dot{m}v_{out} \tag{15}$$

The relationships between the dry air and the vapour stream entering and leaving are:

$$\dot{m}v_{out} = \dot{m}a_{out} * \omega_{out} \tag{16}$$

$$\dot{m}v_{in} = \dot{m}a_{in} * \omega_{in} \tag{17}$$

The energy balance equation, taking into consideration Equation 15, is:

$$\begin{aligned}(\dot{m}v_{in} * h_{in} + \dot{m}a_{in} * h_{in}) + \dot{m}_{c2} * h_{c2} + \dot{m}_{c3} * h_{c3} \\ = \dot{m}_{c1} * h_{c1} + (\dot{m}v_{out} * h_{out} + \dot{m}a_{out} * h_{out})\end{aligned} \tag{18}$$

To simplify the equation, for a unit of dry air, Equation 18 becomes:

$$\left(\frac{\dot{m}v_{in}}{\dot{m}a_{in}} * h_{in} + h_{in}\right) + \frac{\dot{m}_{c2}}{\dot{m}a_{in}} * h_{c2} + \frac{\dot{m}_{c3}}{\dot{m}a_{in}} * h_{c3} = \frac{\dot{m}_{c1}}{\dot{m}a_{in}} * h_{c1} + (\frac{\dot{m}v_{out}}{\dot{m}a_{in}} * \ h_{out} + h_{out}) \tag{19}$$

Using Equations 16 and 17, Equation 19 becomes:

$$(\omega_{in} * h_{in} + h_{in}) + \frac{\dot{m}_{c2}}{\dot{m}a_{in}} * h_{c2} + \frac{\dot{m}_{c3}}{\dot{m}a_{in}} * h_{c3} = \frac{\dot{m}_{c1}}{\dot{m}a_{in}} * h_{c1} + (\omega_{out} * \ h_{out} + h_{out}) \tag{20}$$

$$(\omega_{in} * h_{in}) + \frac{\dot{m}_{c2}}{\dot{m}a_{in}} * h_{c2} + \frac{\dot{m}_{c3}}{\dot{m}a_{in}} * h_{c3} = \frac{\dot{m}_{c1}}{\dot{m}a_{in}} * h_{c1} + (\omega_{out} * \ h_{out}) + (h_{out} - h_{in}) \tag{21}$$

The inflow of dry air is unchanged in the tower but there are water losses due to evaporation, as well as drift losses in droplets carried out of the cooling tower with exhaust air. To prevent scaling and avoid an accumulation of impurities, we blow down an amount of water from the basin. Equation 25 gives the amount of make-up water required (as shown in Figure 15). The mass flow of evaporation is (El-Wakil, 1984):

$$\dot{m}_e = \dot{m}_{air} * (\omega_{out} - \omega_{in}) \tag{22}$$

According to the formulas of Perry and Green (2008), drift losses can be estimated by the following equation:

$$\dot{m}_{drif} = 0.0002 * \dot{m}_{c2} \tag{23}$$

Blow down for mass flow can be considered by the following equation (Perry and Green, 2008):

$$\dot{m}_{bl} = \frac{m_e - (cycles - 1) * \dot{m}_{drif}}{cycle - 1} \quad (24)$$

Finally, the make-up water required is found by the equation:

$$\dot{m}_{c3} = \dot{m}_e + \dot{m}_{drif} + \dot{m}_{bl} \quad (25)$$

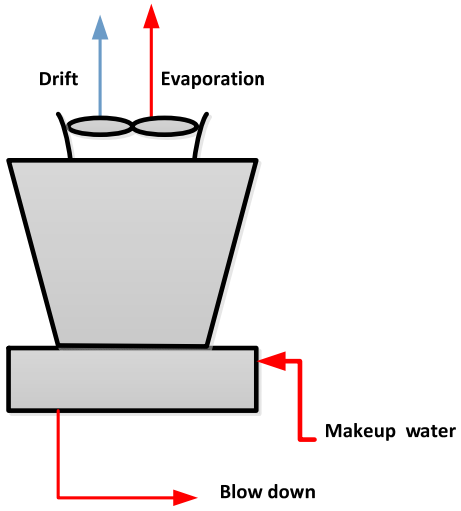

FIGURE 15: Losses in wet cooling systems

Here:
- $\dot{m}a_{in}$ = Mass flow of cold air entering cooling tower (kg/s);
- $\dot{m}a_{out}$ = Mass flow of hot air leaving cooling tower (kg/s);
- $\dot{m}v_{in}$ = Mass flow of water vapour entering cooling tower (kg/s);
- $\dot{m}v_{out}$ = Mass flow of water vapour leaving cooling tower (kg/s);
- $\dot{m}_{c1}$ = Mass flow of water entering condenser (kg/s);
- $\dot{m}_{c2}$ = Mass flow of water leaving condenser (kg/s);
- $\dot{m}_{c3}$ = Mass flow of makeup water entering the cooling tower (kg/s);
- $\dot{m}_e$ = Mass flow of evaporations losses (kg/s);
- $\dot{m}_{drif}$ = Mass flow of drift losses (kg/s);
- $\dot{m}_{bl}$ = Mass flow of blow down losses (kg/s);
- ω_{in} = Humidity ratio of cold air entering cooling tower (kg water/kg dry air);
- ω_{out} = Humidity ratio of hot air leaving cooling tower (kg water/kg dry air);
- h_{in} = Enthalpy of dry air entering cooling tower (kJ/kg);
- h_{out} = Enthalpy of dry air leaving cooling tower (kJ/kg);
- h_{c1} = Enthalpy of cold water leaving cooling tower (kJ/kg);
- h_{c2} = Enthalpy of hot water entering cooling tower (kJ/kg);
- h_{c3} = Enthalpy of makeup water (kJ/kg).

3.6.3 Dry cooling system

Where there is a lack of water supply for the condenser, a dry cooling system can be used. In dry cooling systems, the condenser is a part of the cooling tower, as shown in Figure 16. The condenser is coupled to the exhaust of the turbine to condense the working fluid before entering the pump. This condenser uses the atmosphere as the heat sink.

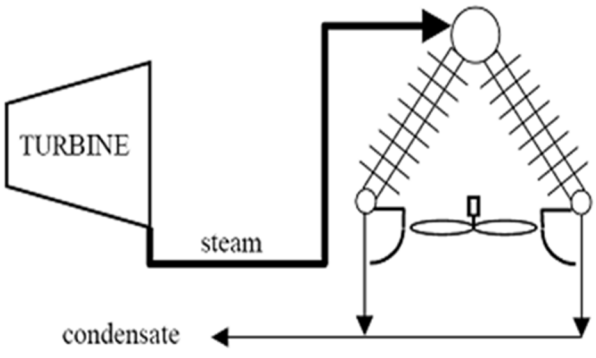

FIGURE 16: The dry cooling system (Renewable Energy in the California Dessert, 2012)

Mostly in geothermal plants, the dry air cooling tower is a mechanical draft type using fans with motors driven by electrical power. Two mechanical fans are used in both a wet cooling system and a dry cooling system (Figure 17):

- The induced draft is a mechanical draft fan on the top of the tower. The main role is to induce the moist air outside with better air circulation across the bundle tube. High power is needed if ambient temperature is high, due to low inlet air velocities.
- The forced draft is a mechanical draft fan on the bottom of the tower, to force air into circulating inside the tower. Air is circulated uniformly in the tower due to the low discharge air velocities

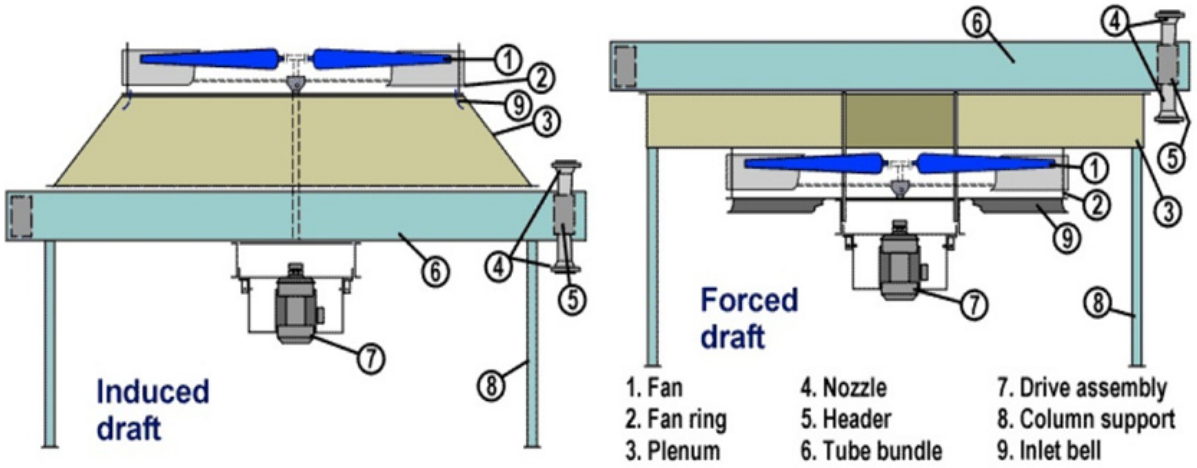

FIGURE 17: Mechanical drafted fan, configuration and components
(Hudson Products Corp., 2004)

from the bundle tube. This type of fan can circulate hot air, but is more impacted by the climatic conditions (i.e. sun, rain), which leads to increased fan maintenance.

The dry cooling system is very sensitive to ambient temperature variations and directly affects the output of the power plant. The dry cooling system in Figure 16 shows the steam going from the turbine to the condenser; after condensation, the condensate goes directly into the cycle. Here, unlike with wet cooling systems, the need for a make-up water supply is eliminated as are water freezing problems, and water vapour plumes. Maintenance and operation requirements and costs are low due to fewer components being used. This is the easiest operation.

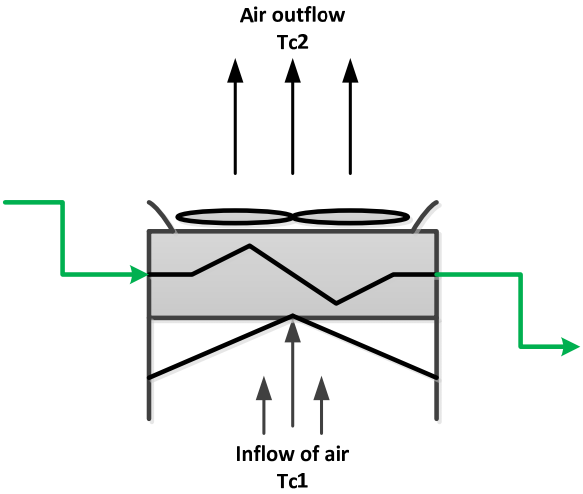

FIGURE 18: A dry cooling condenser

The energy balance in the condenser is represented by the following equation and is pertinent to Figure 18:

$$\dot{m}_{wf} * (h_5 - h_7) = \dot{m}_{air} * cp * (\Delta T) \quad (26)$$

Regarding the temperature difference ΔT between the air entering and leaving the cooling tower, Equation 27 becomes:

$$\dot{m}_{wf} * (h_5 - h_7) = \dot{m}_{air} * cp * (T_{c2} - T_{c1}) \quad (27)$$

where $\dot{m}_{wf}$ = Mass flow of working fluid (kg/s);
$\dot{m}_{air}$ = Mass flow of air flowing inside the condenser (kg/s);
cp = Specific heat (kJ/kg K);
T_{c2} = Temperature of the ambient air leaving the cooling tower (°C);
T_{c1} = Temperature of the ambient air entering the cooling tower (°C).

3.7 Cooling tower components

In both wet cooling and dry cooling, a cooling tower is required as a part of the cooling system. Different components are needed depending on the cooling type, some of which are listed below:

- Frame and casings are employed to support enclosures, motors and fan, and also to collect make-up water from a cold water basin on the bottom of the tower.
- Drift eliminators are used to reduce water droplets in the air stream from the wet cooling system.
- Otherwise, louvers are used to equalize the intake air flow inside the tower and also retain water inside the cooling tower. To facilitate heat transfer by maximizing water and air contact, a filling system is required, and splash fill and film fill are mostly employed (only for wet cooling).
- Nozzles provide water and spray to wet the fill and distribute the water uniformly from the top of the fill in both wet and dry cooling systems.
- Fans are required for different configurations used to circulate air inside the cooling tower.

3.8 Working fluid selection

The working fluid is the fluid used in the ORC cycle. It gets heat from the geothermal fluid and is used in a binary cycle. The selection of the working fluid is very important and has great implications on the performance of the power plant.

The main constraints are the thermodynamic properties of the fluids, as well as considerations of health, safety and environmental impacts (DiPippo, 2008). The working fluid has a lower boiling temperature than water. The most common fluids used are refrigerants and hydrocarbons and, in some cases, mixtures of the two. In this study, we will only consider the working fluid isopentane, the thermodynamic properties of the geothermal brine, and the boundary conditions.

TABLE 1: Properties of isopentane (Lukawski, 2009)

Fluid	Formula	Critical temp., T_c (°C)	Critical pressure, P_c (bar)	Molecular weight, M (g/mol)	Acentric factor ω
Isopentane	$C_5 H_{12}$	187.20	33.78	72.149	0.227

4. COOLING SYSTEM DESIGN

4.1 Selection of cooling systems

For cooling system selection, different parameters must be taken into account to optimize the efficiency of the power plant. Some of the parameters are directly dependent upon weather conditions. The main parameters are listed below:

1. Water availability;
2. Climate, for example air temperature;
3. Effectiveness or performance;
4. Net output or optimal output of the plant;
5. Area of the condenser;
6. Efficiency of the power plant.

4.1.1 Water availability

For each cooling system and power plant, water is a necessary resource. In the North-Goubhet field groundwater is not available for cooling systems. Lake Asal is located in the southwest part of the field (Figure 19), and it is one of the saltiest lakes in the world. In the eastern part of the field, seawater from the Red Sea enters the Goubhet Gulf or Lake Goubhet. The salinity of the seawater is around 42 g/l (NASA Earth Sciences, 2012); this water is considered for the study.

A desalination plant is planned for removal of salinity and oxygen in order to avoid scaling and corrosion problems inside the cooling tower and the piping systems.

4.1.2 Climate data

FIGURE 19: The North-Goubhet area with a focus on water availability

A brief presentation of the climatic situation of the study area is interesting since the climate plays an important role in the cooling system. Djibouti has an arid climate due to its geographic location, being near the equator and open to the warm Red Sea. The climate is characterized by a high level of humidity, and a low pluviometry. In fact, the climate is divided into two main seasons which cover 6 months each. The cold season (Figure 20), which extends from October to March, represents the period when the weather is clement, with temperatures down to 20°C at times, and also with more rainfall than during the warm season. On the other hand, the temperature may differ in the capital and regions in the interior of the country. The hot season extends from April to September, representing the period when high temperatures are recorded. The temperatures can go beyond 45°C with relatively low humidity, although the humidity can be high at the end of the day.

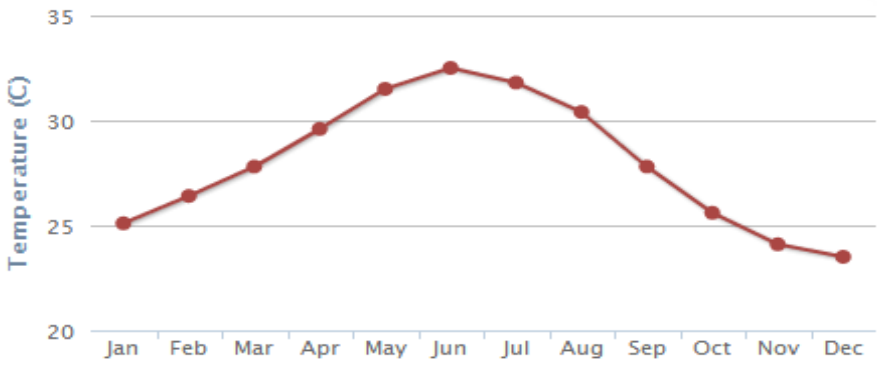

FIGURE 20: Monthly averages of the temperature in Djibouti city in the period 1900-2009 (World Bank, 2012)

The graph with monthly average ambient temperatures presented in Figure 20 shows temperatures varying from 23.5 to 32.5°C. In the summer, high temperatures are recorded in June and July with high humidity as well. In order to show how the temperature varies during a specific day, Figure 21 describes the temperature variations in Djibouti city both during for the hottest day of the year (with a red line) and the coldest day (with a blue line).

The maximum temperature during the hottest day in the summer is around 45°C, but in the cooler season, the lowest temperature is around 20°C. Thus, there is about a 25°C difference between the highest and lowest temperatures. There is a lack of weather data from the North-Goubhet geothermal field. Therefore, data from the city of Djibouti, which is located around 90 km from the geothermal field, are used. Older annual data are not accurate; thus the daily data in Figure 21 are used as a design parameter in the final EES model presented in the report.

4.1.3 Effectiveness and performance

Once the water availability and climatic conditions of the field are determined, the performance of the cooling systems becomes an important parameter for the model. Two factors are used to define the performance, i.e. range and approach. The range is the temperature difference between hot coolant fluids (water or air) entering the cooling tower and the cold coolant fluid leaving the cooling tower. The approach is the temperature difference between the wet bulb air temperature entering the cooling tower and the cold coolant temperature leaving (Figure 22).

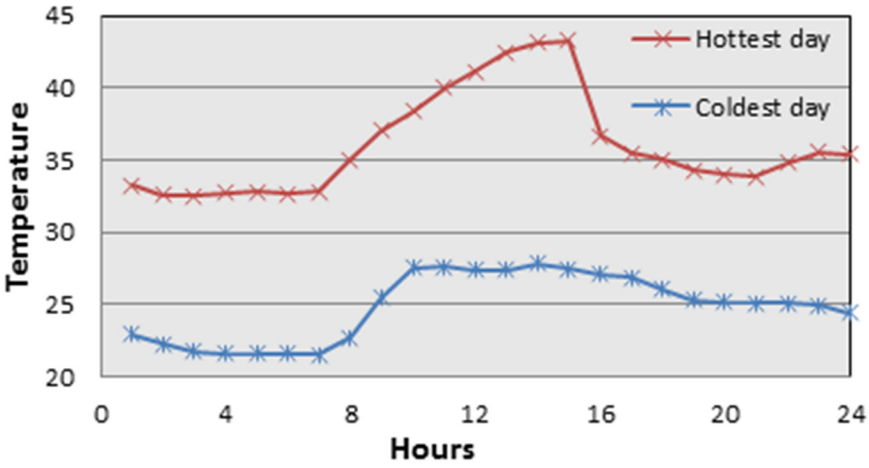

FIGURE 21: Daily temperature curves for Djibouti city for the hottest and coldest day of the year

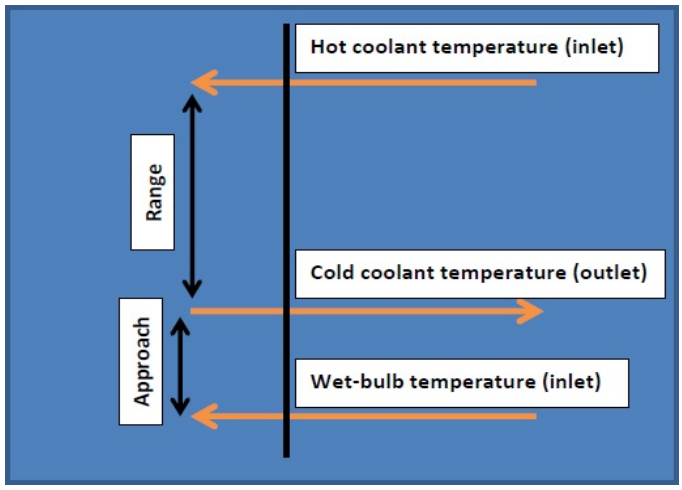

FIGURE 22: Range and approach representation

The performance or effectiveness is the ratio of the actual range to the ideal range, i.e.:

Range / (Range +Approach)

4.1.4 Net output or optimal output of the plant

The net output of the power plant is affected by several components, like preheater and evaporator efficiency. Also, the cooling systems use around 5% of the gross power of the plant. In some cases, cooling tower fans can use around 10-30% of the total gross plant output (Franco and Villani, 2009). The following equations give the net power output of the plant:

$$W_{auxiliary} = P_{pump\ motor} + W_{desalination\ plant} + P_{fan\ motor} \quad (28)$$

$$W_{Net\ output} = W_{turbine} - W_{auxiliary} \quad (29)$$

4.1.5 Area of the condenser

The surface area of the heat exchanger or condenser is totally dependent upon the cooling system chosen. The heat exchanger surface area that is needed represents an important parameter in reducing the cost of the cooling system and for minimizing the total cost of the plant.

4.1.6 Efficiency of the power plant

The cooling system design affects the net output of the power plant and, at the same time, the efficiency of the whole power plant. Efficiency of the plant can be found by considering the first law of thermodynamics, the work produced by the turbine divided by the heat extracted from the geothermal

fluid in the heat exchanger (preheater and evaporator). The total efficiency of the cycle can be found from the following equation:

$$\eta_{cycle} = W_{turbine} / Q_{heat\ exchanger} \quad (30)$$

Here $Q_{heat\ exchanger} = m_{wf} * (h_1 - h_4)$

4.2 Cooling system simulation

4.2.1 Methodology

The study presented in this report includes numerical modelling of two different types of cooling systems, a dry cooling system for a binary cycle (Figure 23) and a wet cooling system, also for a binary cycle (Figure 24).

The following methodology was used in the modelling of the cooling systems:

1. The thermodynamic cycle of the binary plant was developed using the software, Engineering Equation Solver (EES) (F-Chart Software, 2012), focusing on the cooling part of the cycle;
2. Simulations were run with several parameters representing different conditions in the cooling system (condenser);
3. Results of the simulations were analysed in terms of the net output.

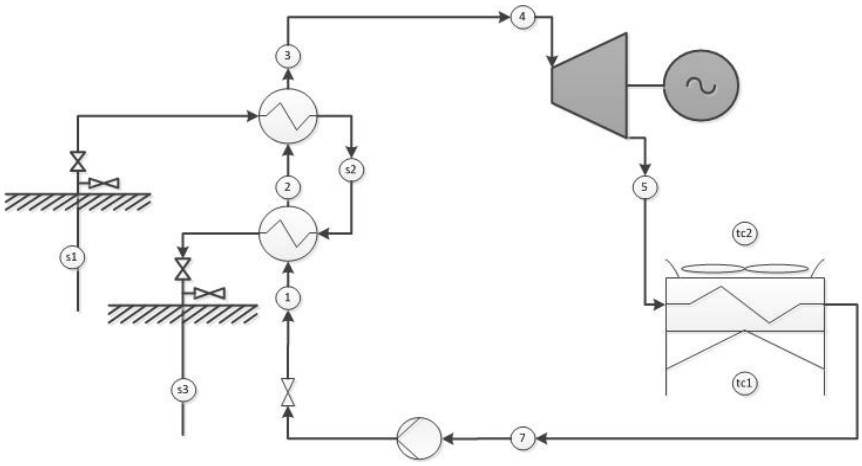

FIGURE 23: Dry cooling system, binary cycle

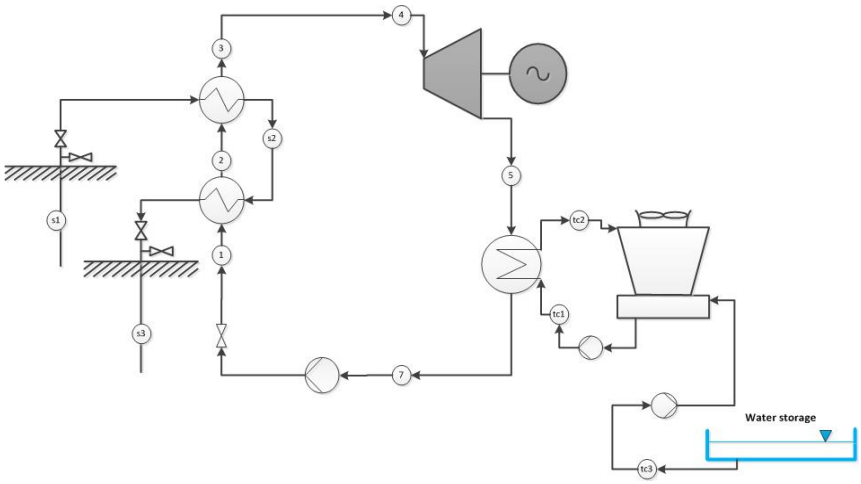

FIGURE 24: Wet cooling system, binary cycle

In this study, several input parameters were estimated as there were insufficient data availability from the field. These assumptions are divided into several parts:

Field data design parameters:

1. The temperature of the geothermal fluid at the wellhead is T = 170°C.
2. The reinjection temperature of geothermal fluid was assumed sufficient to avoid a scaling problem.
3. The mass flow of geothermal fluid was assumed equal to m = 250 kg/s.

4. A dry bulb temperature with a range from 21 to 45°C was used.
5. Seawater from the Red Sea is assumed to be at a temperature between 22 and 35°C; the median temperature is equal to 28.5°C for the reference design.

Efficiency of components:

1. The efficiency of the turbine $\eta_{turbine}$= 0.85.
2. The efficiency of the pump η_{pump}= 0.75.
3. The efficiency of the fan η_{fan}= 0.80.
4. The efficiency of the motor of the fan η_{motor}= 0.85.

Pinch temperature:

1. A superheated cycle was considered and $T_{superheater}$ = 2°C.
2. The pinch point $T_{pinch\_vaporizer}$ = 3°C.
3. The pinch point $T_{pinch\_condenser}$ = 4°C.

Psychometric properties of the air:

1. The relative humidity of the air leaving the cooling tower was assumed to be 90% in the wet cooling case.
2. Median air temperature is 33°C and is considered as the design parameter with 50% relative humidity.
3. In a wet cooling system, air temperature leaving the tower was assumed equal to the temperature entering plus 14°C.

Overall heat transfer coefficient for condenser:

1. $U_{Condensing}$= 0.35 kW/(m^{2}K) for condensing process for dry air cooling system (Engineering Toolbox, 2012).
2. $U_{Condenser}$= 0.2 kW/(m^{2}K) for desuperheated process for dry air cooling system (Engineering Toolbox, 2012).
3. $U_{Condensing}$= 1.4 kW/(m^{2}K) for condensing process for wet cooling system.
4. $U_{Condenser}$= 0.7 kW/(m^{2}K) for desuperheated process for wet cooling system.

ORC cycle factor:

1. The ORC cycle used was a simple model with a single-pressure turbine and isopentane as the working fluid.
2. The vaporizer pressure of the working fluid was assumed equal to *P_vaporizing* = 20 bars.
3. The most important part was the cooling system, so two systems were considered for this study:
   - The air cooled or dry cooling system;
   - The wet cooling system.

All these parameters composed the boundary conditions for this study. Some parameters were arbitrarily set to simplify the study due to a lack of available data.

4.2.2 Results of the simulation

Appendix I shows the EES simulation models, both for the dry cooling system and the wet cooling system. The influence of different parameters on the cooling systems is discussed below.

Influence of ambient air temperature:

The outside temperature or ambient air is an important parameter for a cooling system design, both for dry cooling and wet cooling. To demonstrate this influence, a simulation was run for a range of ambient temperatures for different relative humidity, and the net output of the power plant was then calculated.

Figure 25 shows the net output of the plant for dry cooling systems and Figure 26 shows the net output for wet cooling. In both cooling systems, the ambient air temperature affects the net output of the plant. However, the ambient air temperature affects the dry cooling system more than the wet cooling system. The output of the dry cooling system decreases by around 30% from the lowest temperature to the highest. Ambient air is the principal coolant in the dry cooling system, so it impacts directly the net output of the plant. But if the humidity is higher, increases from 50 to 70% relative humidity, the power produced does not vary so much (violet line in Figure 25).

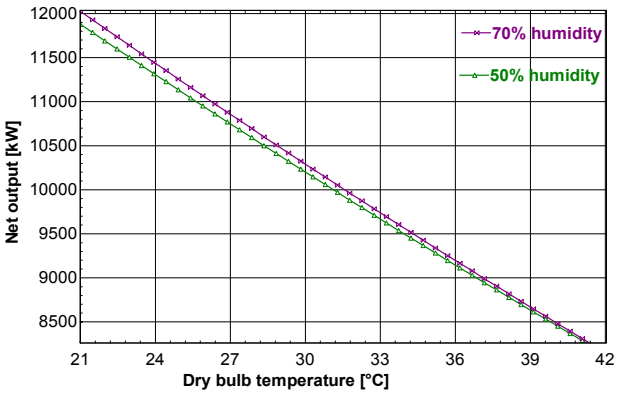

FIGURE 25: Net output as a function of ambient air temperature for a dry cooling system

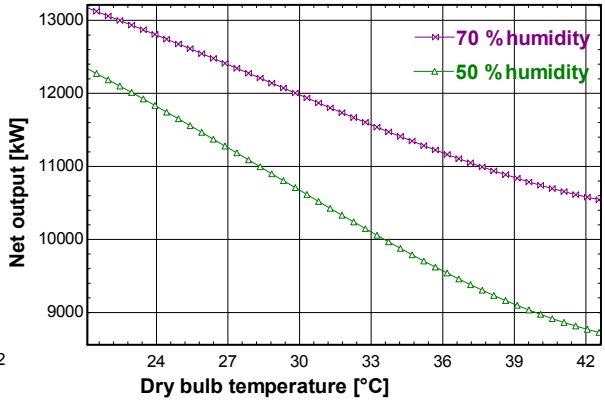

FIGURE 26: Net output as a function of ambient air temperature for a wet cooling system

For a wet cooling system the humidity response is greater. As shown in Figure 26 a large difference is found in the net output between 50 and 70% relative humidity of the inlet air. Further net output decrease would be expected if the ambient air humidity decreases more, e.g. to 25%. High humidity content in the air leads to less impact of the air temperature on the net output of the power plant.

Make-up water requirement in the wet cooling system:

Make-up water is only required in the wet cooling system, to compensate for losses due to evaporation, drift losses, and blow down. The water supply to the cooling tower comes from the desalination plant. Thus, the water supply plays an important part in the cost of the plant and impacts directly the cooling process. Figure 27 shows the mass flow of make-up water required if the ambient air temperature goes from 21 to 45°C. If the ambient temperature increases, the evaporation losses will also increase. To fill these losses, more make-up water is needed to supply the cooling tower, almost double the amount in the example shown in Figure 27. Evaporation losses account for 70% of the total losses, blow down for 29%, and drift for less than 1%.

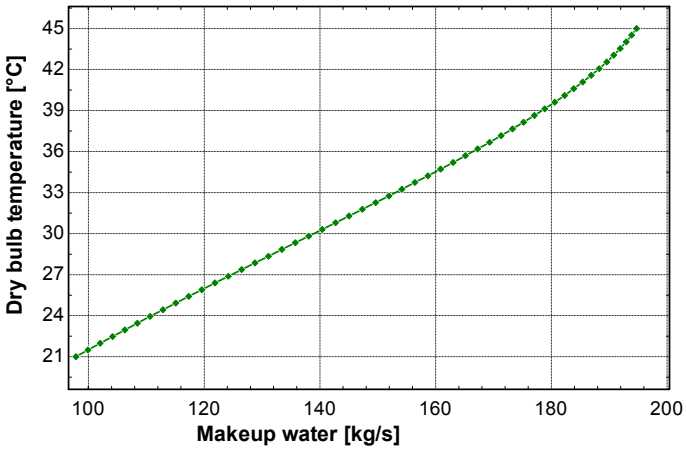

FIGURE 27: Make-up water in a wet cooling system

Blow down depends on the number of cycles (3 in this study) of concentration. In cooling towers with high cycles of concentration the blow down loss is kept limited but more impurities are encountered in the cooling tower. This leads to an increased need for chemical treatments to prevent impurities in the tower basin (Zhai and Rubin, 2010).

Condenser surface area:
When finding the optimum cooling system, the area of the proposed condenser is an important parameter which influences strongly the cost of the condenser. Figure 28 shows a dry cooling condenser area. This system needs a huge surface area in comparison with the wet cooling condenser area (Figure 29). Almost 4 times bigger condenser surface area is required in the dry cooling system.

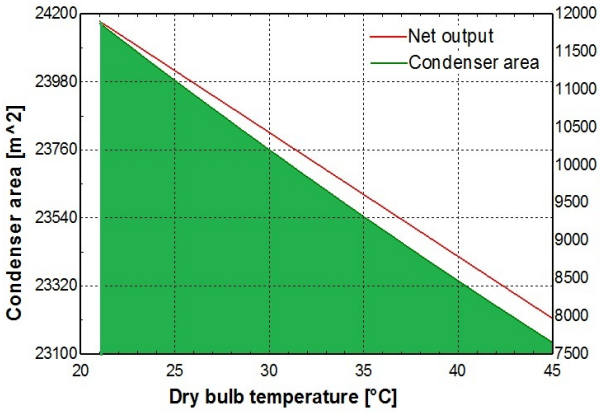

FIGURE 28: Surface condenser area for dry cooling

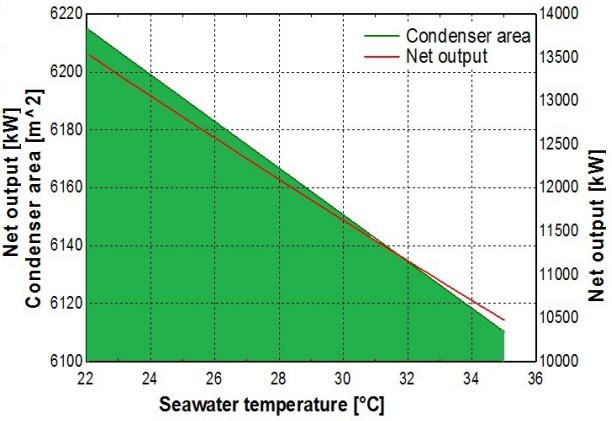

FIGURE 29: Surface condenser area for wet cooling

As already pointed out the wet cooling system uses less condenser surface area or about 6000 m² (Figure 29), and ambient temperature does not affect the wet cooling system like it does in the dry cooling system. The wet cooling system is mainly affected by the seawater temperature, ranging from 22 to 35°C, as shown in Figure 29. In a wet cooling system, an increase in seawater temperature leads to a reduction in the condenser's surface, corresponding to a decrease in the net output (Figure 29, red line). In the EES simulation for a constant seawater temperature, where ambient air temperature increases, the area of the condenser does not evolve so much. However, in a dry cooling system, the ambient air is the principal coolant fluid entering the condenser, so the evolution of the temperature has an important impact.

The condenser area corresponds to the net output of the plant. The red lines in Figures 28 and 29 show the net output decreasing at the same time as the area of the condenser is reduced. Water has almost 830 times higher density than air. The heat transfer coefficient is higher for water, so more air volume than water is needed for cooling, thus influencing the surface of the condenser.

Efficiency of the plant:
Simple binary plants have a thermal efficiency between 10 and 15% (DiPippo, 2008). Following the previous arguments and using the equation defining the efficiency, the results are shown in Figure 30.

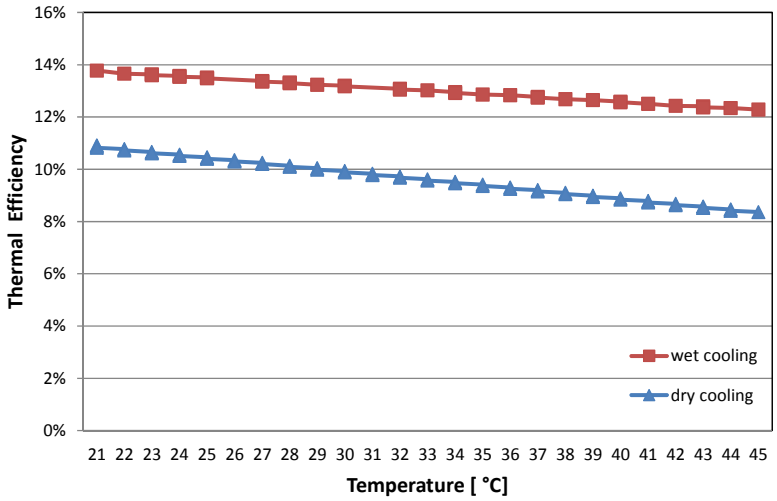

FIGURE 30: Conversion efficiency as a function of ambient air temperature

The temperature of the water entering the condenser in a wet cooling system impacts the efficiency of the plant and, if this temperature increases, the efficiency of the plant reduces

drastically. The efficiency ranges between 14 and 10%, with a decrease associated with higher ambient air temperature for both cooling systems. The wet cooling system has a higher thermal efficiency than the dry cooling system as shown in Figure 30, with around 2% difference.

4.2.3 Cost analysis of the power plant

The cost of a geothermal power plant has become more competitive than other energy technologies, but the high investment cost in drilling is still an obstacle. Figure 31 summarises the cost of the different components of a geothermal plant project. The power plant cost represents around 39% of the total cost of the project, including a cooling system (wet cooling case). About 7% is allowed for exploration studies. The costs represent an obstacle for large developments. Also, the utilization of different fluids (geothermal fluid, working fluid, water) and the efficiency of the plant are limiting factors. The cooling system also represents an important part of the cost of the plant and, in some specific conditions, it can represent up to 30 or 35% of the capital cost of the geothermal project (Franco and Villani, 2009).

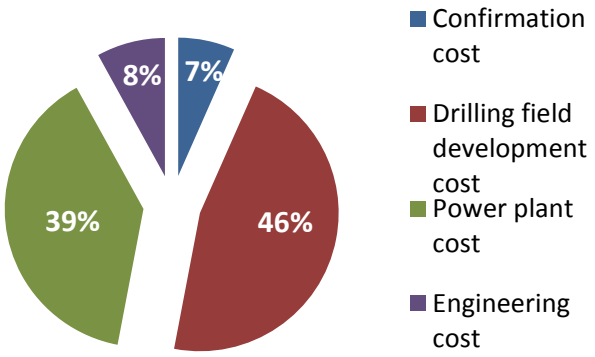

FIGURE 31: Capital cost distribution of a geothermal power plant (ÍSOR, 2012)

Table 2 shows the estimated cost of different components such as a condenser, the feeding pump required for wet and water cooling systems and a desalination plant. Figure 32 is based on the cost values given in Table 2. The data in Table 2 come mostly from several UNU students' reports and some recent papers. Observations are based on the premise that wet cooling systems require less area for a condenser than dry cooling systems.

TABLE 2: Cost components of a cooling system (USD)

Geothermal cost analysis	Dry cooling	Wet cooling	Water cooling
Condenser (USD/m²)	600[1]	156.8[2]	78.404[2]
Cooling tower (USD/kW)	0	30[2]	0
Desalination plant (USD/m³)	0	2000[3]	2000
Pump (USD/kW) *only feeding pump on cooling part*	0	500[2]	500[2]

Price per unit: [1](Nazif, 2011); [2]Lukawski, 2009; [3]Cost estimated according to local project

The wet cooling costs include the cost of different components like a feed pump, cooling tower, and a desalination plant for make-up water. The cost of a desalination plant is an estimated capital cost for a plant with an average capacity of pure water production of around 1000 m^3, used mainly for make-up water due to losses. Pump works are considered in the cost analysis and the head of discharge is estimated based on the topography of the field.

The preliminary cost analysis show high capital cost required for a dry cooling system, due to the huge condenser surface area needed. The cost for a dry cooling system is around 2 times higher than the cost for a wet cooling system (Figure 32). In wet cooling, the cost of a cooling tower represents around 60% of the total cost of the cooling system while the desalination plant accounts for around 20%. The capital cost of water infrastructures, as well as a storage tank, pumps and a supply pipeline from the desalination plant to the power plant are not considered in this study, but would increase the total cost of the cooling system.

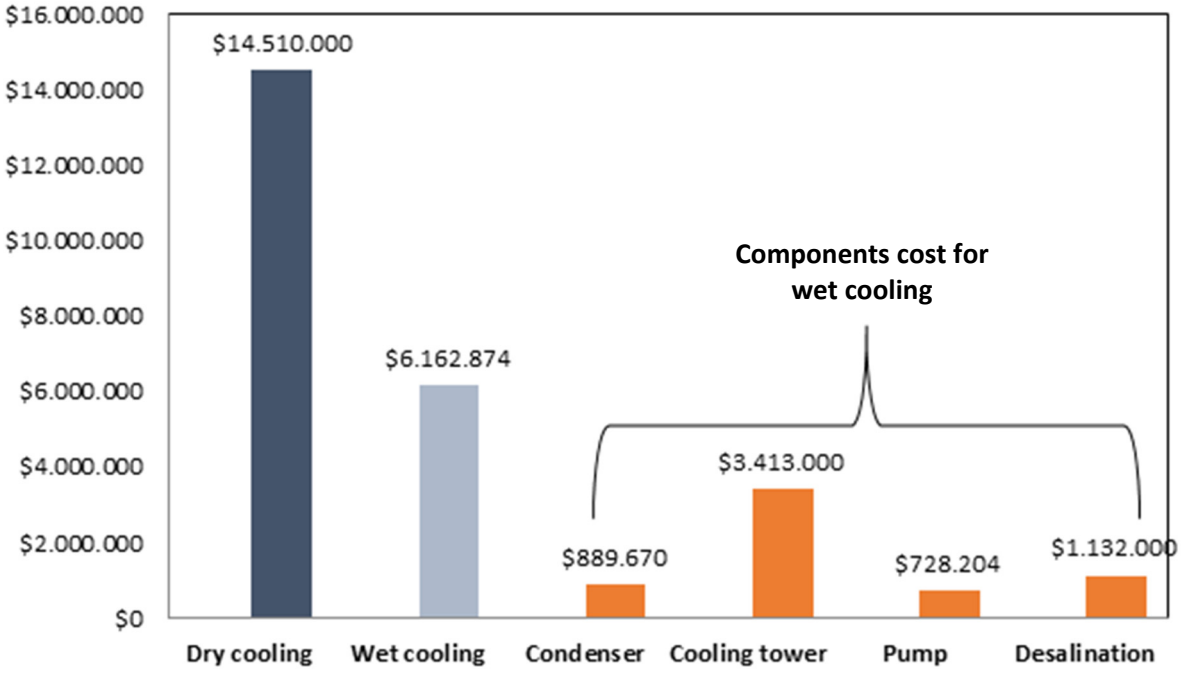

FIGURE 32: Cost evolution for wet and dry cooling systems (USD)

5. CONCLUSIONS

A cooling system is an important parameter in binary plant design, and this report has tried to give some information on how one can design and select the optimal cooling system.

In the study, the focus is on a simple binary cycle in the North-Goubhet geothermal field in Djibouti. Based on the results from the newest survey done by CERD in 2010, a geothermal resource in this field was clearly identified with a temperature estimated at 170°C by geothermometers. Based on this information, a binary plant was designed for power generation. With regard to the extreme climatic conditions of the area, and to improve the efficiency of the plant, the focus was on the cooling system design.

During this brief study, three different cooling systems available for geothermal binary cycles were examined, water cooling, wet cooling and dry cooling. The study identified different parameters for each design.

Due to groundwater or surface water unavailability in the proposed area, only two cooling systems were selected for further study: wet cooling and dry cooling. According to the design parameters, several simulations were done using EES simulation software. The most important parameters were the temperature of the ambient air, efficiency, and the surface of the condenser. A cost analysis model was developed.

The results show that a wet cooling system requires many components and a more complex cycle than the dry cooling system. In terms of efficiency of the cycle the wet cooling system gives the best results but it is affected by variations in the temperature of the seawater.

This study shows that the most competitive cooling system in the North-Goubhet geothermal field for a small geothermal power plant is a dry cooling system due to the psychometric properties of the ambient air, necessary investment costs, and thermal efficiency.

6. RECOMMENDATIONS

Available data on the North-Goubhet field is limited. Therefore, it would be very interesting to study further and estimate more accurately the potential and characteristics of the geothermal reservoir, such as enthalpy, temperature, pressure and other important parameters. An exploratory drilling survey is planned for 2013 to confirm the resource and the potential.

For dry cooling system calculations, parasitic consumption can be included and taken into account in order to find the effective output of the plant. The temperature of the air leaving the cooling tower must be taken into account according to the CTI (Cooling Technology Institute). Additionally, the optimum temperature at the outlet of the cooling tower must be found to ensure the best plant performance.

ACKNOWLEDGEMENTS

First of all, I would like to express my deepest gratitude to the United Nations University Geothermal Training Programme UNU-GTP and the management board of the Ministry of Energy and Water in charge of Natural Resources in Djibouti for this opportunity to attend and participate in the 34th session of the UNU-GTP in the Geothermal Utilization course.

I wish to thank sincerely the management team of UNU-GTP, Dr. Ingvar Birgir Fridleifsson, director of UNU-GTP, Mr. Lúdvík S. Georgsson, deputy director, Ms. Thórhildur Ísberg, Ms. Málfrídur Ómarsdóttir, Mr. Ingimar G. Haraldsson and Mr. Markús A.G. Wilde. I also take this opportunity to thank all the UNU fellows and my colleagues on the engineering team for our precious friendship during my stay in Iceland.

This work was finalized with the guidance and invaluable assistance from my supervisors, Mr. Árni Ragnarsson, engineer at ISOR and Mr. Indridi Ríkhardsson, assistant professor at Reykjavik University.

Finally, my great thanks go to my mother, Ms. Aicha W. Farah, my father, Mr. Khaireh A. Hared, for their constant prayers and to all my family for their constant support during my stay in Iceland.

REFERENCES

Barberi F., Ferrara G., Santacroce R., and Varet J., 1975: Structural evolution of the Afar triple junction. *Proceedings of the Conference "Afar Depression of Ethiopia", Bad Bergzarben, F.R. Germany*.

BRGM, 1983: *Geothermal prospection in the North-Ghoubhet field with gravimetry and AMT survey (Republic of Djibouti)* (in French). BRGM, France, report 83 GPH014, 27 pp.

CERD, 2010: *Prefeasibility study for North-Ghoubhet field, Republic of Djibouti* (in French). CERD, Djibouti, unpublished report, 58 pp.

CFG, 1985: *Geothermal project Asal-Ghoubbet, updating notes on 15th May 1985* (in French). CFG, Djibouti 23 pp.

DiPippo, R., 2008: *Geothermal power plants. Principles, applications, case studies and environmental impact*. Elsevier Ltd., Kidlington, UK, 493 pp.

El-Wakil, M.M., 1984: *Power plant technology*. McGraw-Hill, Inc, USA, 859 pp.

Engineering Toolbox, 2012: *Heat transfer coefficients in heat exchangers.* Engineering toolbox, website: *www.engineeringtoolbox.com/heat-transfer-coefficients-exchangers-d_450.html.*

F-Chart Software, 2012: *EES, Engineering equation solver.* F-Chart Software, website: *www.fchart.com/ees/ees.shtml.*

Franco, A., and Villani, M., 2009: Optimal design of binary cycle power plants for water-dominated, medium temperature geothermal fields. *Geothermics, 38*, 379-391.

Geothermica, 1987: *Geochemistry of North Goubhet-Asal region,* Geothermica Italiana Srl, Pisa, ISERST report, 28 pp.

Hudson Products Corp., 2004: Performance improvement to existing air-cooled heat exchangers. *Presented at the 2004 Cooling Technology Institute (CTI) Annual Conference, Houston*, 16 pp.

ÍSOR, 2012: *Binary plant capital cost estimate.* Iceland GeoSurvey – ÍSOR, Reykjavik, unpublished data.

Jalludin, M., 2012: State of knowledge of geothermal exploration, Republic of Djibouti. *Presented at Energy Workshop, University of Djibouti*, unpublished lecture.

Lukawski, M., 2009: *Design and optimization of standardized organic Rankine cycle power plant for European conditions*. University of Akureyri, MSc thesis, 76 pp.

Mendrinos, D., Konloleontos. E., and Karystas, C., 2012: *Geothermal binary plants: water or air cooled?* LOW-BIN Geothermal Power, EC supported project, webpage: *www.lowbin.eu/public/CRES-GeothermalBinaryPlants-Water%20or%20Air%20Cooled.pdf*

NASA Earth Sciences, 2012: *Salinity.* NASA, USA, website: *science.nasa.gov/earth-science/oceanography/physical-ocean/salinity.*

Nazif, H., 2011: Feasibility of developing binary power plants in the existing geothermal production areas in Indonesia. Report 29 in: *Geothermal training in Iceland 2011.* UNU-GTP, Iceland, 709-735.

Perry, B.H., and Green, D.W., 2008: *Perry's chemical engineers' handbook.* McGraw-Hill, Inc., NY, 2735 pp.

Renewable Energy in the Californian Desert, 2012: *Dry cooling.* Renewable Energy in the Californian Desert, website: *webservices.itcs.umich.edu/drupal/recd/?q=node/150.*

Tapponnier P., and Varet, J., 1974: The Makarassou zone in the Afar area: equivalent to emerged faults transforming into ocean (in French). *C. R. Acad. Sc. Paris, 278, Série D,* 209-212.

Wikipedia, 2012: *Surface condenser*. Wikipedia, website: *en.wikipedia.org/wiki/Surface_condenser.*

World Bank, 2012: *Climate change knowledge portal*. World Bank, website: *sdwebx.worldbank.org/climateportal/index.cfm.*

Zhai, H., and Rubin, E.S., 2010: Performance and cost of wet and dry cooling systems for pulverized coal power plants with and without carbon captured and storage. *Energy Policy, 30,* 5653-5660.

APPENDIX I:

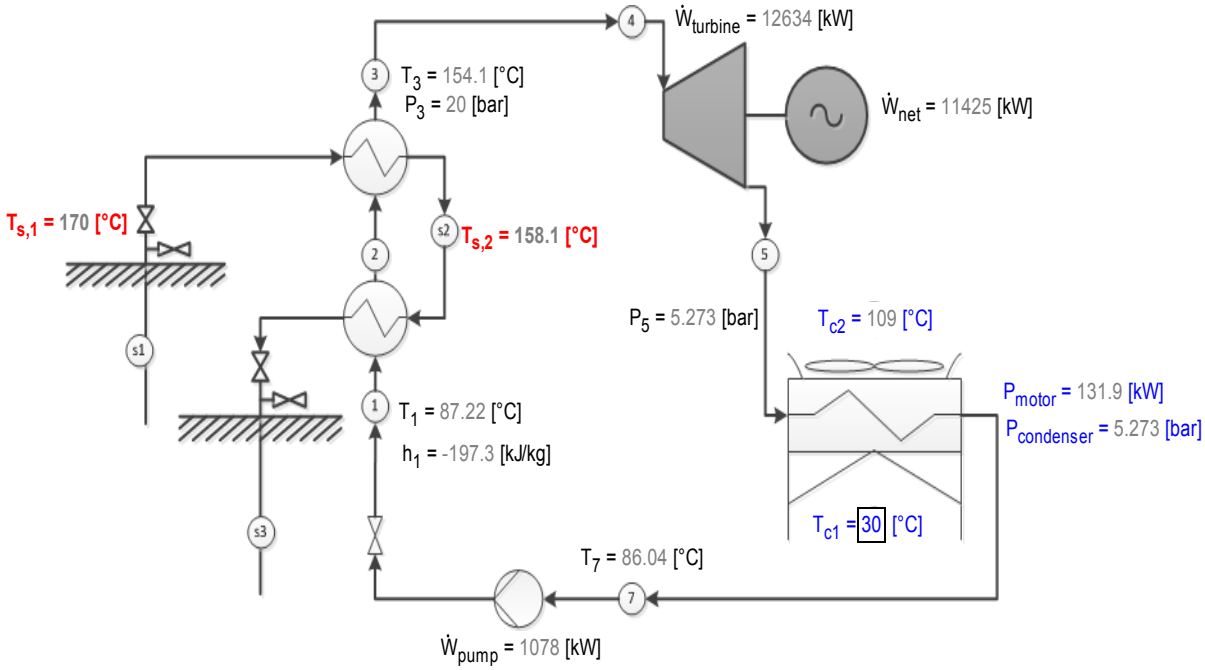

FIGURE 1: Dry cooling system, EES simulation

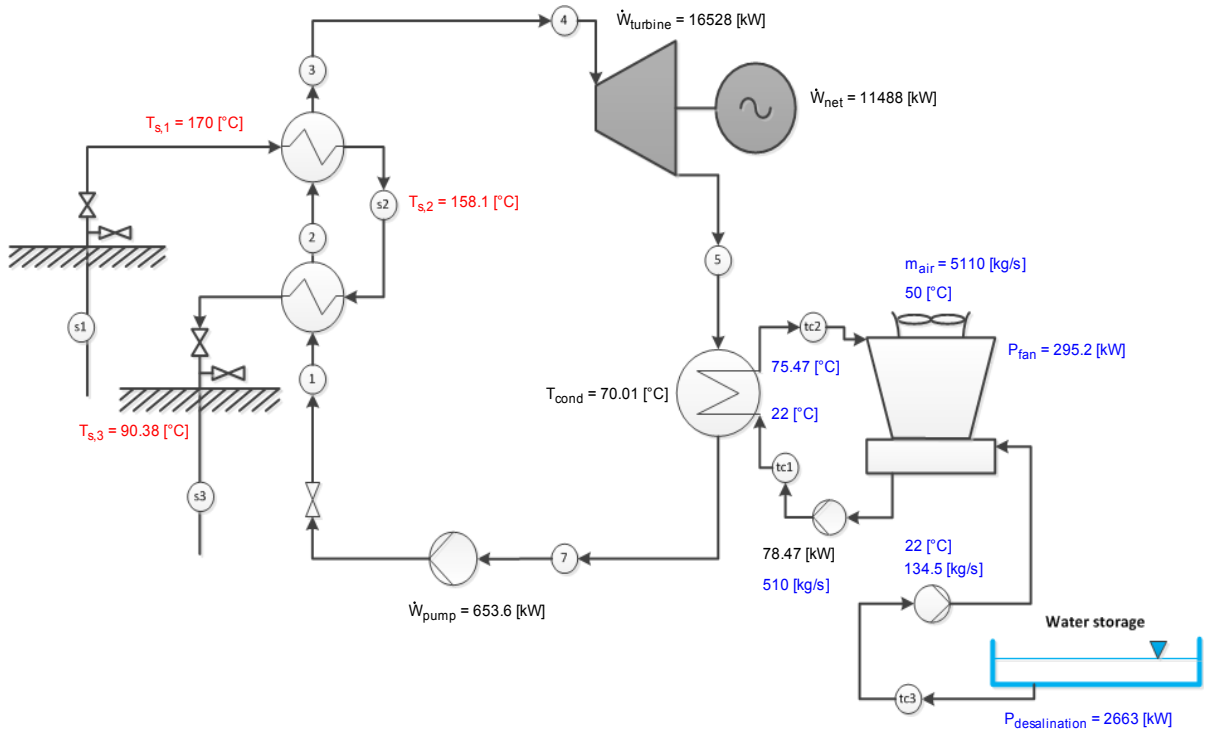

FIGURE 2: Wet cooling system, EES simulation